

Soft Switching Scheme for Three Phase Three Level Dc-Dc Converter with Asymmetrical Duty Cycle Control



G.Sowjanya
M.Tech Student,

Nova College of Engineering, Vijayawada, India.



B.Vinod Kumar, M.Tech
Associate Professor,

Nova College of Engineering, Vijayawada, India.

ABSTRACT:

This paper proposes development of soft switching scheme for three phase three level DC-DC converter for different duty cycles to achieve ZVS for all switches. The ZVS is achieved with output inductor and leakage inductor of transformer. This paper describes the main operational modes of proposed converter for different duty cycle and simulation results are observed and compare the switching losses of proposed converter with and without ZVS.

KEYWORDS:

Zero Voltage Switching (ZVS), Three Phase Three Level (TPTL), DC-DC converter, Pulse width modulation, Duty cycle, Soft switching.

I. INTRODUCTION:

In high voltage high power applications the ordinary converters exist many problems like stress on switches, switching losses, EMI etc.... These problems can be eliminated by using ZVS and ZCS converters. In ZVS, the switches are turned on and off at zero voltages and in ZCS, the switches are turned on and off at zero currents. As a result power reduces almost to a least value, by which the stress on the switches can be reduced. Full-bridge dc/dc converters have been widely used in medium to high power applications to further reduce the stress on switches for high power application TPTL was proposed. With three phase architecture the converter has the superior features including lower current rating of switches reducing input output current ripple allowing small size filter requirement. Although predominant characteristics exist in TPTL soft switching has not been achieved which limits the switching frequency and power loss. The use of Asymmetrical duty cycle in the three phase three level dc/dc converter was proposed in order to achieve ZVS commutation over a wide load range.

II. PROPOSED TPTL DC/DC CONVERTER FOR DIFFERENT DUTY CYCLES:

Fig. 1 shows the circuit configuration of TPTL converter in which, a three-phase transformer with Δ -Y connection is employed for the smaller turn's ratios and transformer VA rating. As shown, L_{ra} , L_{rb} and L_{rc} are the additional resonant inductances to widen the ZVS commutation load range. L_{lka} , L_{lkb} , and L_{lkc} are the equivalent primary leakage inductances of each phase. D_{f1} and D_{f2} are free-wheeling diodes. C_{ss} is the flying capacitor, which is in favor of decoupling the switching transition of Q_1, Q_3, Q_4 , and Q_6 . $DR_1 - DR_6$ are rectifier diodes. The output filter is composed of L_f and C_f , and R_L is the load. Fig. 2 shows the control strategy of proposed converter. To realize the soft-switching for switches, the original interleaved switches should be designed in a complementary manner, and a short delay time t_d is necessary to be introduced between the two complementary switches to provide an interval for the ZVS commutation, which is similar to the control strategy of asymmetrical half-bridge converter. Accordingly, the duty cycles of Q_1, Q_3 , and Q_5 are served to regulate the output voltage, while the drive signals of Q_4, Q_6 , and Q_2 are complementary to that of the Q_1, Q_3 , and Q_5 , respectively.

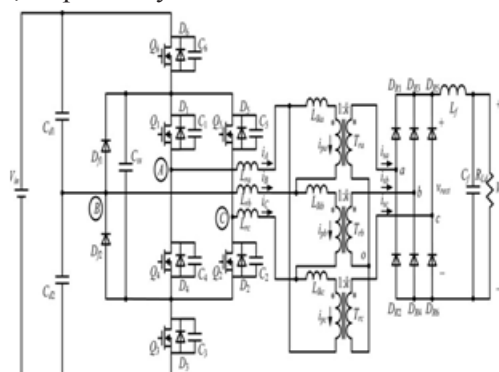


Fig 1: Topology configuration of TPTL dc/dc converter.

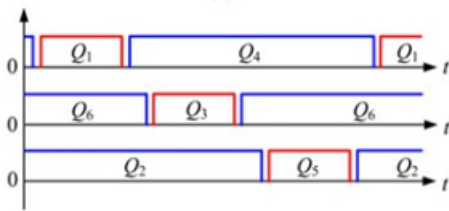


Fig 2: Asymmetrical duty cycle control.

III. OPERATION OF PROPOSED TPTL CONVERTER:

This section will analyze the operation principles of the TPTL converter under the modified control scheme. The following assumptions are made for the simplicity before the analysis:

- 1) all power devices and diodes are ideal;
- 2) all capacitors and inductances are ideal;
- 3) the output filter inductance is large enough to be treated as a constant current source during a switching period; its value equals to output current
- 4) the inductances of each phase are identical, i.e., $L_{lka}=L_{lkb}=L_{lkc}=L_{lk}$, $L_{ra}=L_{rb}=L_{rc}=L_r$;
- 5) $C_1 = C_2 = C_3 = C_4 = C_5 = C_6 = C_p$.

Fig. 3 shows the key waveforms of the TPTL converter with asymmetrical duty cycle control, as seen, the operation of the TPTL converter can be classified by different modes, according to the duty cycle range and the load current. The corresponding operation modes are defined as the small duty cycle mode (SDCM), and the large duty cycle mode (LDCM).

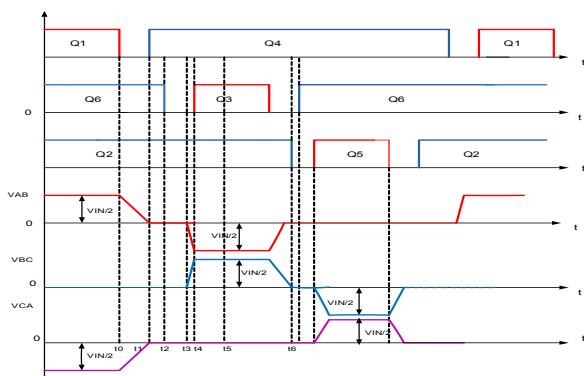


Fig 3: Key waveforms of the TPTL converter with asymmetrical duty cycle control with SDCM.

The basic equations of the voltages and currents of the transformer are listed as follows:

$$V_{AB} + V_{BC} + V_{CA} = 0 \quad (1)$$

$$i_{sa} + i_{sb} + i_{sc} = 0 \quad (2)$$

$$\frac{dia}{dt} = k \frac{(disa)}{dt} = \frac{vLlka}{Llk}, \frac{dipb}{dt} = k \frac{(disb)}{(dt)}$$

$$= \frac{vLlkb}{Llk}, \frac{(dipc)}{dt} = k \frac{(disc)}{dt} = \frac{vLlkc}{Llk} \quad (3)$$

Where k represents the secondary-to-primary turns ratios of the transformer. The voltage across the leakage inductance of transformer can be derived from (2) and (3) and is given as follows

$$V_{Llka} + V_{Llkb} + V_{Llkc} = 0. \quad (4)$$

Stage1[0 -t0]:

Fig.4(a) Shows Q1, Q2, Q6, and Df2 are conducting at the primary side, and DR1 and DR6 are conducting at the secondary side. $V_{AB} = V_{in} / 2$, $V_{BC} = 0$, and $V_{CA} = -V_{in} / 2$. From (1), (2), (4), and other constraints between voltages and currents of transformers, the following expressions can be obtained.

$$V_{pa} = \frac{V_{in}}{2}, V_{pb} = 0, V_{pc} = -\frac{V_{in}}{2} \quad (5)$$

$$V_{rect} = V_{sa} - V_{sc} \cdot k \cdot V_{in} \quad (6)$$

Where V_{pi} and V_{si} are the primary voltage and secondary voltage of transformers, i represents the subscripts a, b, and c.

Stage 2[t0- t1]:

Fig.4 (b) Shows At t_0 , Q1 is turned off, the line current i_a charges C1 and discharges C4 linearly, and the rectified voltage decreases. As C1 limits the rising rate of the voltage across Q1, Q1 is zero-voltage turn-off. The voltages across C1 and C4 are

$$V_{c1}(t) = \frac{1}{C_p} k I_o (t - t_0) \quad (7)$$

$$V_{c4}(t) = \frac{V_{in}}{2} - \left(\frac{1}{C_p} k \cdot I_o (t - t_0) \right) \quad (8)$$

At t_1 , v_{C1} rises to $V_{in}/2$, and V_{C4} decays to zero; therefore, D_4 conducts naturally, and V_{rect} decreases to zero.

Stage 3 [$t_1 - t_2$]:

Fig.4(c) Shows after C_1 is fully charged, the current flowing through C_1 transfers to C_{ss} and begins to charge C_{ss} . The voltage across C_{ss} will increase and block D_2 to be off. During this stage, $V_{AB} = V_{BC} = V_{CA} = 0$. D_4 conducts and clamps the voltage across Q_4 at zero, so Q_4 can be turned on at zero-voltage condition. DR_1 and DR_6 conduct, and V_{rect} is still zero.

Stage 4 [$t_2 - t_3$]:

Fig.4 (d) Shows At t_2 , Q_6 is zero-voltage turned-off and V_{AB} increases reversely. If v_{pk} keeps constant, the polarity of the voltage applied on L_{lk} will be non associated with the current flowing through L_{lk} ; as a result, i_p will decrease and cannot provide the load current, then DR_3 begins to conduct, and the current commutation between DR_1 and DR_3 occurs. In the primary stage, C_3 and C_6 resonate with the leakage inductances and the resonant inductances, and the following expressions will be obtained.

$$V_{c3}(t) = \frac{V_{in}}{2} - \left(\frac{1}{2}\right)k \cdot I_o \cdot Z_r \cdot \sin[\omega r(t - t_2)] \quad (9)$$

$$V_{c6}(t) = \left(\frac{1}{2}\right)k \cdot I_o \cdot Z_r \cdot \sin[\omega r(t - t_2)] \quad (10)$$

$$i_{A(t)} = \frac{3}{2}k \cdot I_o + \frac{1}{2}k \cdot I_o \cos[\omega r(t - t_2)] \quad (11)$$

$$i_{B(t)} = -k \cdot I_o \cos[\omega r(t - t_2)] \quad (12)$$

$$i_{C(t)} = -\frac{3}{2}k \cdot I_o + \frac{1}{2}k \cdot I_o \cdot \cos[\omega r(t - t_2)] \quad (13)$$

During this stage, V_{rect} remains at zero. When V_{c3} decays to zero, D_3 conducts naturally.

Stage 5 [$t_3 - t_4$]:

Fig.4 (e) Shows As D_3 is conducting, the voltage across Q_3 is clamped at zero; therefore, Q_3 is turned on at zero-voltage condition. During this stage, Q_2, Q_3 , and Q_4 conduct in the primary stage, $V_{AB} = -V_{in}/2$, $V_{BC} = V_{in}/2$, and $V_{CA} = 0$. DR_1, DR_3 , and DR_6 conduct in the secondary stage, and $V_{rect} = 0$. From (1), (2), (4), and other constraints between voltages and currents of transformers, the expressions of the phase currents are given in (14)–(16)

$$i_{pa}(t) = i_{pa}(t_3) - \frac{V_{in}}{2L_p} \cdot (t - t_3) \quad (14)$$

$$i_{pb}(t) = i_{pb}(t_3) + \frac{V_{in}}{2L_p} \cdot (t - t_3) \quad (15)$$

$$i_{pc}(t) = -kI_o \quad (16)$$

Therefore, the line currents can be obtained from (14) to (16)

$$i_{A(t)} = i_{A(t_3)} - \frac{V_{in}}{2L_p} \cdot (t - t_3) \quad (17)$$

$$i_{B(t)} = i_{B(t_3)} + \frac{V_{in}}{L_p} \cdot (t - t_3) \quad (18) \quad i_{C(t)} = i_{C(t_3)} - \frac{V_{in}}{2L_p} \cdot (t - t_3) \quad (19)$$

At the secondary stage, I_s flows through DR_1 and decreases with i_{pa} from (14). When I_s decreases to zero, DR_1 turns off and DR_2 conducts. It should be noted that the rectified voltage is lost during the interval $t_3 - t_4$, compared with the primary line voltage. Therefore, the duty cycle loss in SDCM is defined as

$$D_{loss1} = \frac{t_{34}}{T_s} = \frac{6k \cdot I_o \cdot L_p}{V_{in} \cdot T_s} \quad (20)$$

Where T_s is the switching period.

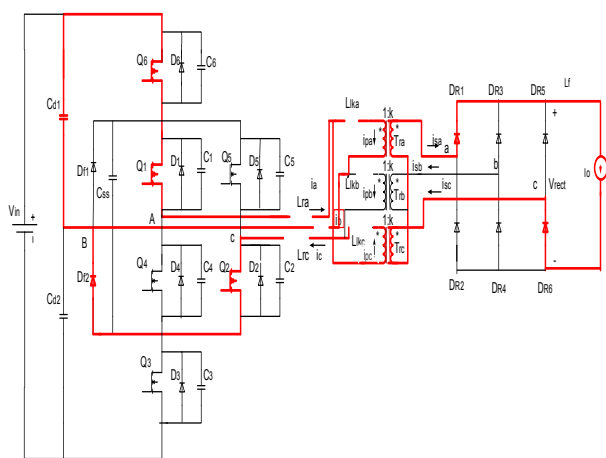
Stage 6 [$t_4 - t_5$]:

Fig.4 (f) Shows During this stage, $V_{AB} = -V_{in}/2$, $V_{BC} = V_{in}/2$, $V_{CA} = 0$.

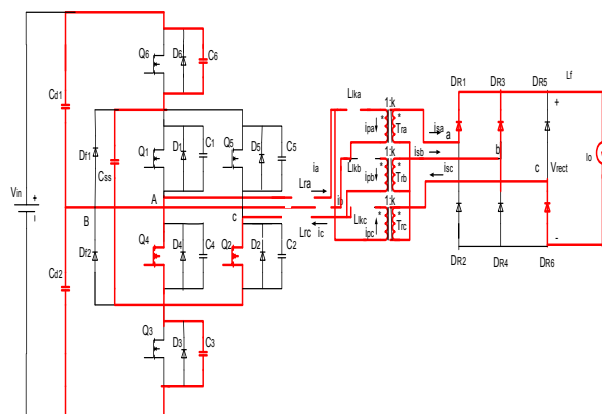
I_s flows through DR_6 , i_{sc} and decreases with i_{pc} . When i_{sc} decreases to zero, DR_6 turns off, the primary and secondary currents of transformer T_{rc} are both zero. The time interval of this stage is given by $t_{45} = (4k \cdot I_o \cdot L_p) / V_{in}$ (21)

Stage 7 [$t_5 - t_6$]:

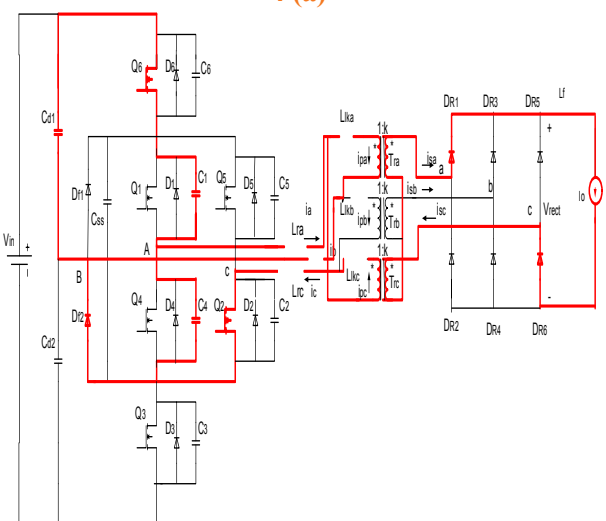
Fig.4 (f) Shows Q_2, Q_3 , and Q_4 conduct at the primary side, while DR_2 and DR_3 conduct at the secondary side, and the rectified voltage is kV_{in} , which is similar to the stage 1.



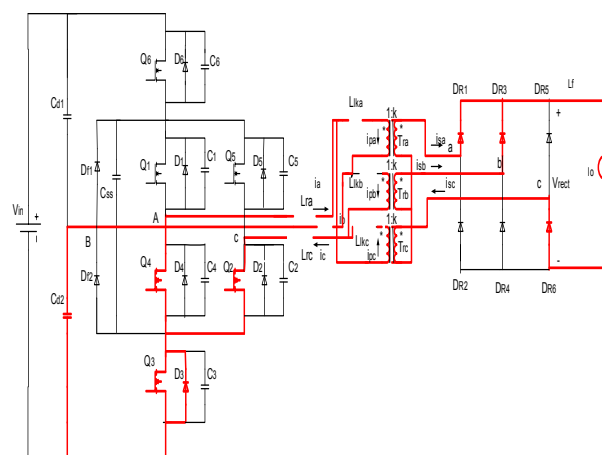
4 (a)



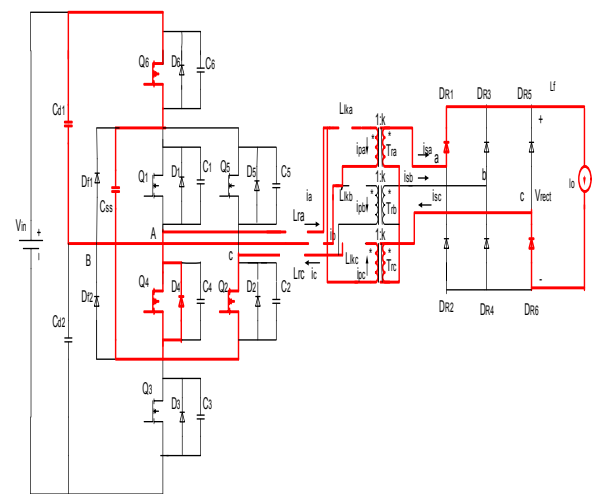
4 (d)



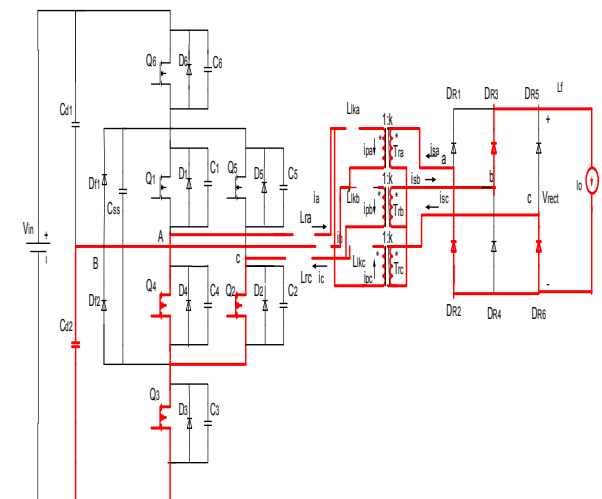
4(b)



4 (e)



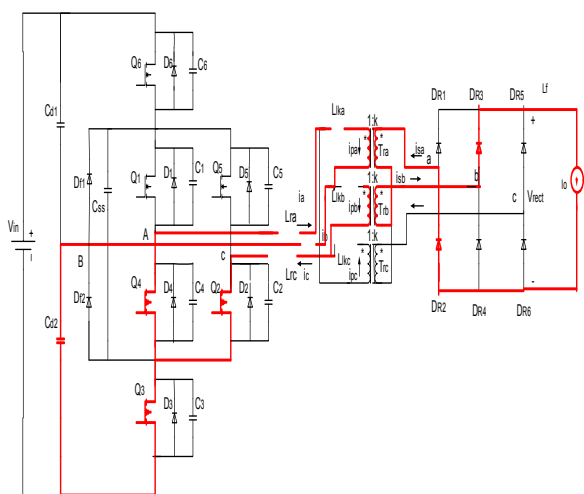
4 (c)



4 (f)

Fig 4: Equivalent circuits under different operation stages (d) [t2, t3]. (e) [t3, t4]. (f) [t4, t5]

Fig 4: Equivalent circuits under different operation stages. (a) Prior to[0 t0] . (b) [t0, t1]. (c) [t1, t2]



4 (g)

Fig 4: Equivalent circuits under different operation stages (g) [t5, t6]

IV.SIMULATION RESULTS FOR THREE PHASE THREE LEVEL DC/DC CONVERTER:

In fig.5 Simulink model of a 200V/16V DC-DC converter has been proposed. In fig.6.output waveforms of the proposed converter is shown. In the proposed converter there is total six switches out of it Q1,Q3,Q5 are given with same duty cycle and Q2,Q4,Q6 are same having same duty cycle.

Though the switches have same duty cycle all the switches not on for the same time In the proposed converter there are total six switches in which all are under goes soft switching for different duty cycles Fig.7 & Fig.8 shows the simulation results for D=20%.

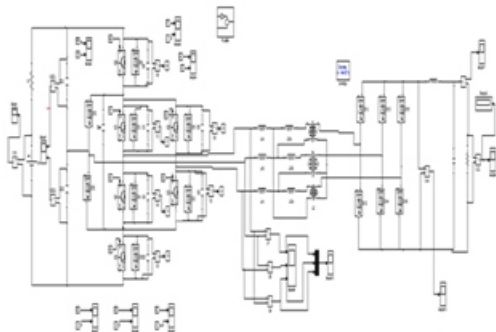


Fig 5: Simulink diagram of three phase Three-Level DC-DC converter

As the duty cycle increases the output voltage will increase as shown in Table 1. In which the output voltage will increase from D=20% to 46% and efficiency also increases. Fig6 represents output waveforms of the converter and three phase output voltage also observed in which all the phases are shifted by 120°. Fig7 represents soft switching of the proposed converter for Q1 and Q4 switches. Which is also same for Q2,Q3,Q5,Q6. Fig.7a shows voltage across Q1, fig 7b.shows the ZVS for Q1 from off to on & fig7c shows on to off of Q1 under the ZVS. Fig 8a shows voltage across Q4, fig 8b.shows the ZVS for Q4 from off to on & fig 8c.shows on to off of Q4 under the ZVS. Fig9 shows graph between efficiency and load current at duty cycle D=20%, which will also represent the efficiency is high for with soft switching than without soft switching.

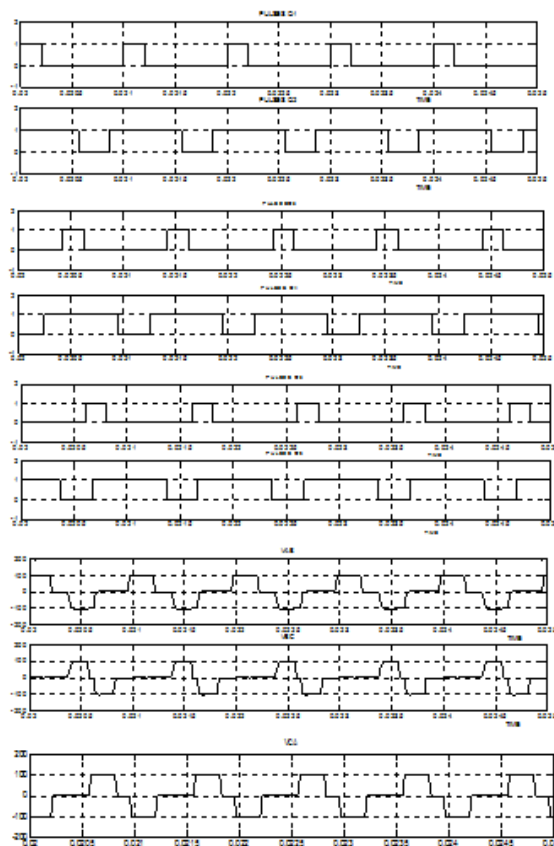


Fig 6: output waveform Simulation results for Duty cycle 20% Voltage across Q1

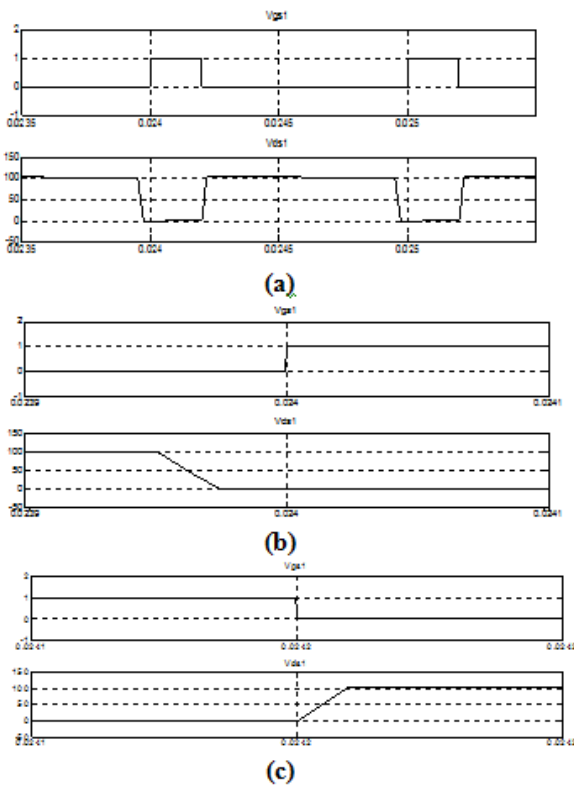


Fig7: for 20% duties cycle (a) voltage across switch Q1, (b). zvs turn off-on Q1(c)zvs turn on-off Q1.

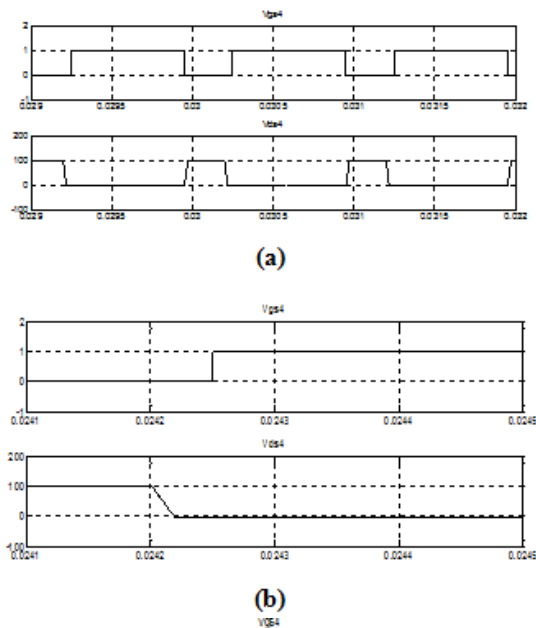


Fig8: for 20% duty cycles (a) voltage across switch Q4, (b). zvs turn off-on Q4(c) zvs turn on-off Q4.

TABLE1:

Duty cycle (%)	Output voltage (V)	Efficiency with soft switching (%)	Efficiency without soft switching (%)
15	6.56	51.78	38.29
20	11.7	64.67	44.1
30	13.95	69.81	50.36
40	15.33	71.45	54
48	15.8	81.87	57.77

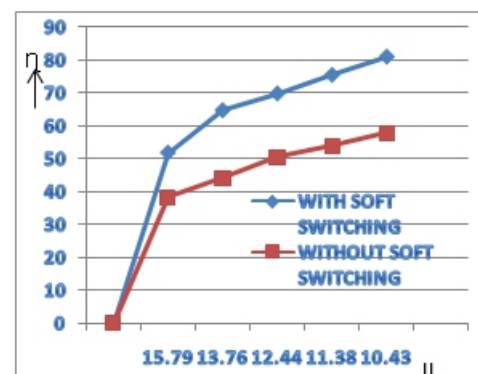


Fig 9: Load current Vs Efficiency at D=20%

IV. CONCLUSION:

Soft switching scheme is achieved in each and every switch. Voltage stress across each switch was reduced. By increasing the voltage levels the size of the filter elements may also reduce. The switching losses in the proposed converter are reduced. The proposed control scheme features the following characteristics:

- 1) Compared with the hard switching technique the losses in switches predominately reduced

2) The input capacitors can realize automatic and inherent voltage balancing, which ensures that all the switches sustain only one-half of the input voltage. 3) The TPTL converter will operate in different duty cycles.

REFERENCES:

[1] F. Liu, G. Hu, and X. Ruan, "Three-phase three-level DC/DC converter for high input voltage and high-power applications-adopting symmetrical duty cycle control," *IEEE Trans. Power Electron.*, vol. 29, no. 1, pp. 56–65, Jan. 2014.

[2] D. V. Ghodke, K. Chatterjee, and B. G. Fernandes, "Modified soft switched three-phase three-level DC–DC converter for high-power applications having extended duty cycle range," *IEEE Trans. Ind. Electron.*, vol. 59, no. 9, pp. 3362–3372, Sep. 2012.

[3] D. V. Ghodke, K. Chatterjee, and B. G. Fernandes, "Three-phase three level, soft switched, phase shifted PWM dc-dc converter for high power applications," *IEEE Trans. Power Electron.*, vol. 23, no. 3, pp. 1214–1227, May 2008.

[4] J. Jacobs, A. Averberg, and R. De Doncker, "A novel three-phase DC/DC converter for high-power applications," in *Proc. IEEE Power Electron. Spec. Conf.*, 2004, pp. 1861–1867.

[5] H. Cha and P. Enjeti, "A novel three-phase high power current-fed DC/DC converter with active clamp for fuel cells," in *Proc. IEEE Power Electron. Spec. Conf.*, 2007, pp. 2485–2489.

[6] A. K. S. Bhat and R. L. Zheng, "A three-phase series-parallel resonant converter-analysis, design, simulation, and experimental results," *IEEE Trans. Ind. Appl.*, vol. 32, no. 4, pp. 951–960, Jul./Aug. 1996.

[7] R. W. De Doncker, D. M. Divan, and M. H. Kheraluwala, "A three phase soft-switched high-power-density DC/DC converter for high-power applications," *IEEE Trans. Ind. Appl.*, vol. 27, no. 1, pp. 63–73, Jan./Feb. 1991.

[8] P. D. Ziogas, A. R. Prasad, and S. Manias, "Analysis and design of a three phase off-line DC/DC converter with high frequency isolation," in *Proc. IEEE Ind. Appl. Soc. Annu. Meeting*, 1988, pp. 813–820. [9] H. Kim, C. Yoon, and S. Choi, "A three-phase DC–DC converter for fuel cell applications," in *Proc. IEEE Power Electron. Spec. Conf.*, 2008, pp. 1290–129.

Authors Details:

G. Sowjanya She completed her B. Tech in electrical and electronics engineering from PNC&VIET, Guntur, in the year 2012. Currently she pursuing M. Tech in Power electronics and drives from Nova College of engineering, Vijayawada.

B. Vinod Kumar Received the B. Tech from Sir C R REDDY College of engineering and technology (Electrical & Electronics Engineering), Eluru, West godhavari, M. Tech from Nimra College of engineering and Technology, Jupudi, Krishna. Currently he is working as an Assoc. Professor in Dept. of EEE in Nova College of engineering, Vijayawada.